Expanded View Figures

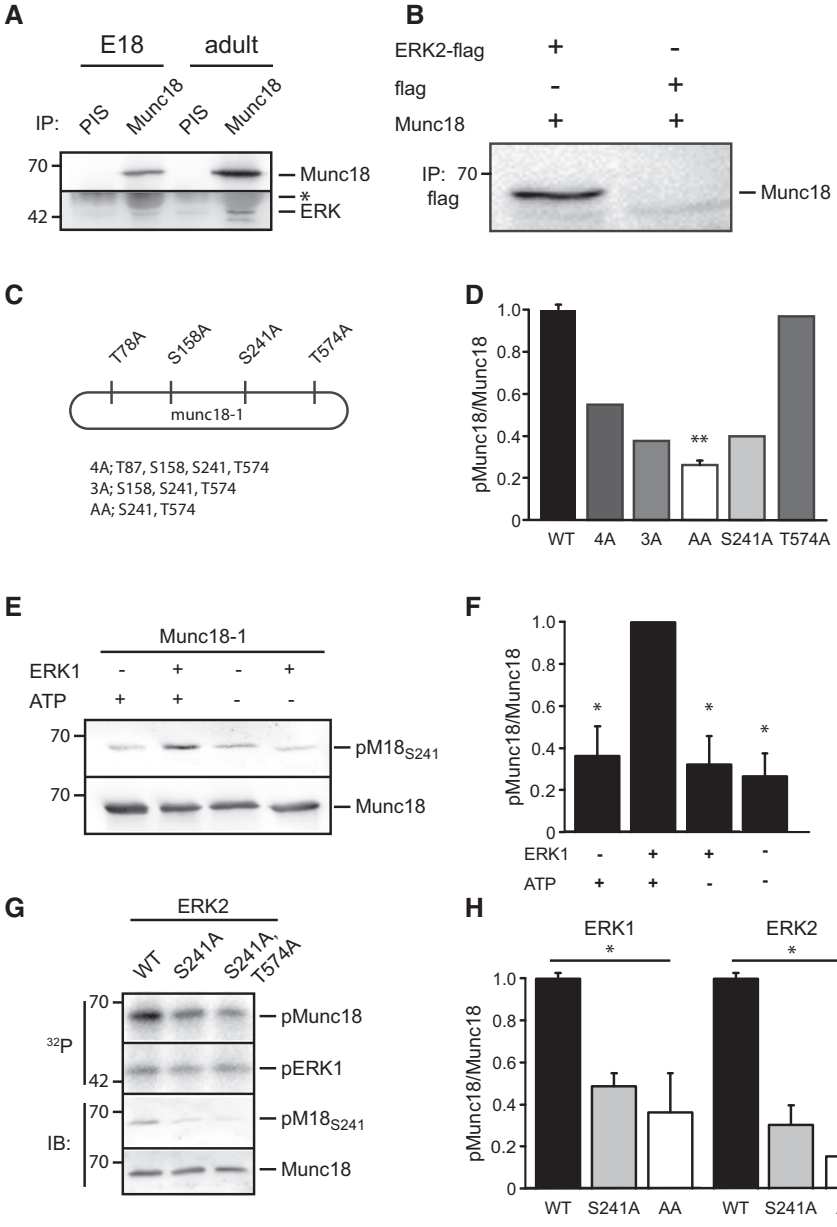

Figure EV1. ERK1/2 binds and phosphorylates Munc18-1.

Related to Figure 1.

A, B Binding between Munc18-1 and ERK in brain and in HEK293T cells. (A) Co-immunoprecipitation (IP) of ERK and Munc18-1 from embryonic (E18) or adult brain lysate with Munc18-1 antibody, but not with pre-immune serum (PIS). The immunoglobulin heavy chain is visible (*) above the ERK band. (B) Co-immunoprecipitation from HEK293T cells transfected with Munc18-1 and ERK2-flag or empty-flag (as negative control) with flag antibody. Western blot is stained for Munc18-1.

C Diagram of Munc18-1 showing 4 potential ERK phosphorylation sites (P-X-S/T-P). These sites were mutated to alanine yielding 4A (T87A, S158A, S241A, and T574A), 3A (S158A, S241A, and T574A), AA (S241A and T574A), T574A and S241A.

D Quantification of radioactive phospho-Munc18-1 intensity in different Munc18-1 mutants from Fig 1B. Phosphorylation was measured as the amount of ^{32}P incorporation in Munc18-1 normalized to total Munc18. Phosphorylation of $Munc18_{WT}$ was set as 100% ($Munc18_{WT}$: 100 ± 3%, n = 3; $Munc18_{4A}$: 55%, n = 1; $Munc18_{3A}$: 38%, n = 1; $Munc18_{AA}$: 24 ± 2%, n = 3, $^{**}P < 0.01$; $Munc18S_{241A}$: 36%, n = 1; $Munc18_{T574A}$: 100%, n = 1), one-way ANOVA.

E–H Test of phospho-specific $Munc18_{S241}$ antibody. (E) *In vitro* ERK kinase assay, HEK293T cells were transfected with biotinylated Munc18-1. Protein complexes were precipitated with streptavidin-coated magnetic beads and subjected to *in vitro* ERK kinase assay with recombinant ERK1. Western blots were stained with a phospho-specific antibody directed against pS241 ($pM18_{S241}$) and Munc18-1 antibody. (F) Quantification of (E). Phosphorylation was measured as ratio of $pM18_{S241}$ over total Munc18. Condition ERK1 plus ATP was set as 100% (n = 3, $^{*}P < 0.05$), one-way ANOVA. (G) *In vitro* ERK kinase assay, HEK293T cells were transfected with $M18_{WT}$, $M18_{S241A,T574A}$, and $M18_{S241A}$. Munc18-1 variants were immune-precipitated and subjected to *in vitro* kinase assay with recombinant ERK2. Radioactive phosphoblot and immunoblot of *in vitro* ERK kinase assay are stained with $pM18_{S241}$ and Munc18-1 antibody. (H) Quantification of phosphorylation as $pM18_{S241}$ intensity in (G) normalized to total Munc18. Phosphorylation of $M18_{WT}$ was set to 100% (n = 3 for ERK1 and ERK2 *in vitro* assays, $^{*}P < 0.05$), one-way ANOVA.

Data information: Data are expressed as mean ± SEM.

© 2016 The Authors

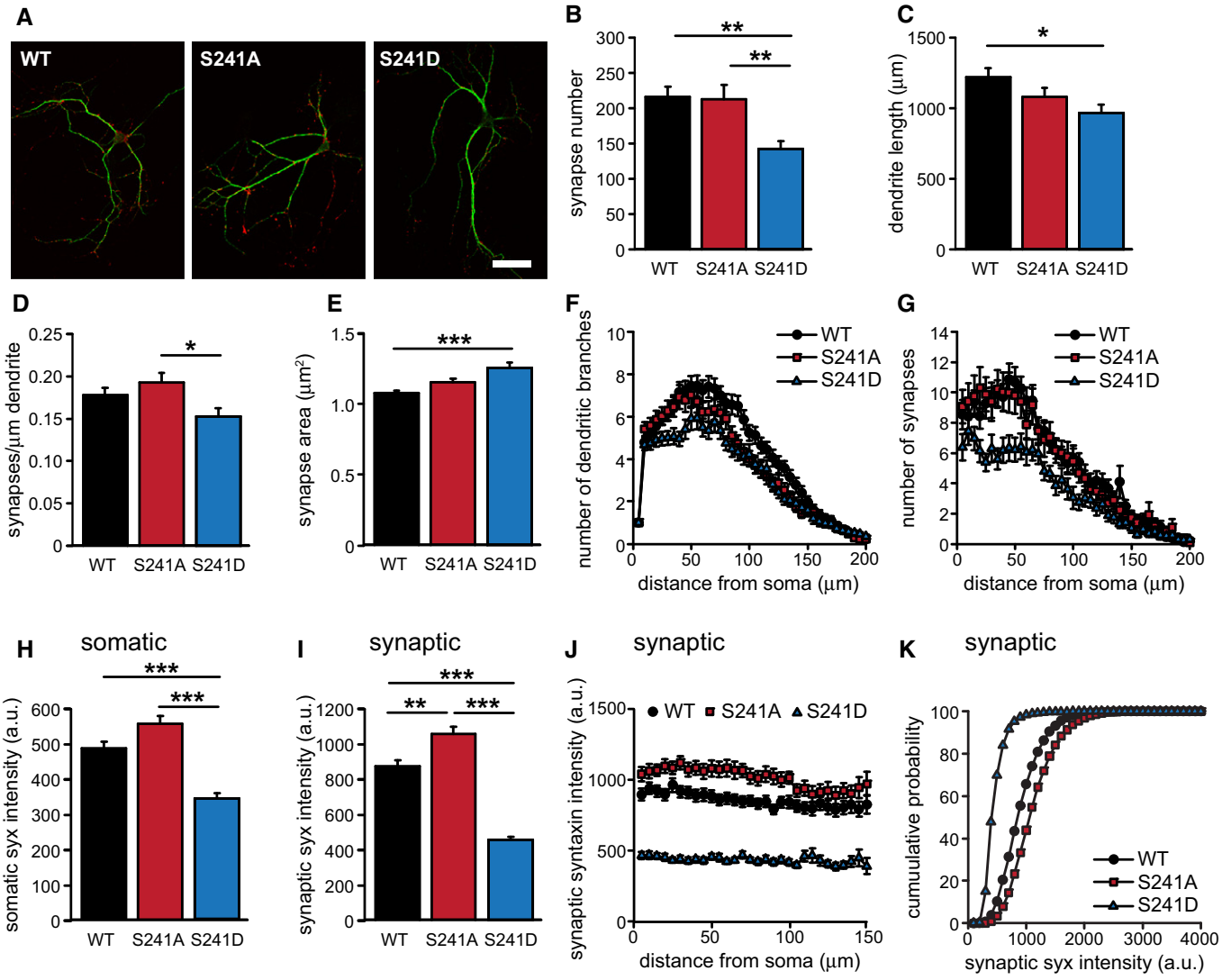

Figure EV2. Neuronal morphology of rescued Munc18-1 null mutant cells.

Related to Figure 4. Hippocampal autaptic neurons of Munc18-1 null mutant mice were rescued with lentiviruses expressing $M18_{WT}$, $M18_{S241A}$, or $M18_{S241D}$ and stained for dendritic MAP2, synapse marker VAMP2, and syntaxin.

A Typical examples. MAP2 (green), VAMP2 (red). Scale bar represents 50 µm.

B Mean synapse number per cell ($M18_{WT}$: 216 ± 15, n = 51; $M18_{S241A}$: 214 ± 21, n = 46; $M18_{S241D}$, one-way ANOVA: 143 ± 11, n = 40; $^{**}P < 0.01$, one-way ANOVA).

C Mean dendrite length per cell ($M18_{WT}$: 1226 ± 61 µm, n = 51; $M18_{S241A}$: 1084 ± 65 µm, n = 46; $M18_{S241D}$: 971 ± 59 µm, n = 40; $^{*}P < 0.05$, one-way ANOVA).

D Number of synapses per µm dendrite length ($M18_{WT}$: 0.179 ± 0.008, n = 51; $M18_{S241A}$: 0.193 ± 0.012, n = 46; $M18_{S241D}$: 0.153 ± 0.010, n = 40; $^{*}P < 0.05$, one-way ANOVA).

E Mean synapse area ($M18_{WT}$: 1.08 ± 0.02 µm², n = 51; $M18_{S241A}$: 1.16 ± 0.03 µm², n = 46; $M18_{S241D}$: 1.26 ± 0.04 µm², n = 40; $^{***}P < 0.001$, one-way ANOVA).

F Number of dendritic branches as a function of radial distance from the soma quantified by Sholl analysis.

G Number of synapses as a function of radial distance from the soma.

H Mean somatic syntaxin intensity ($M18_{WT}$: 485 ± 19, n = 49; $M18_{S241A}$: 554 ± 23, n = 46; $M18_{S241D}$: 343 ± 14, n = 39; $^{***}P < 0.001$, one-way ANOVA).

I Mean synaptic syntaxin intensity ($M18_{WT}$: 875 ± 35, n = 51; $M18_{S241A}$: 1,058 ± 42, n = 46; $M18_{S241D}$: 458 ± 19, n = 40; $^{**}P < 0.01$; $^{***}P < 0.001$, one-way ANOVA).

J Mean synaptic syntaxin intensity as a function of radial distance from the soma.

K Cumulative probability plot of synaptic syntaxin intensity.

Data information: Data are expressed as mean ± SEM.

© 2016 The Authors

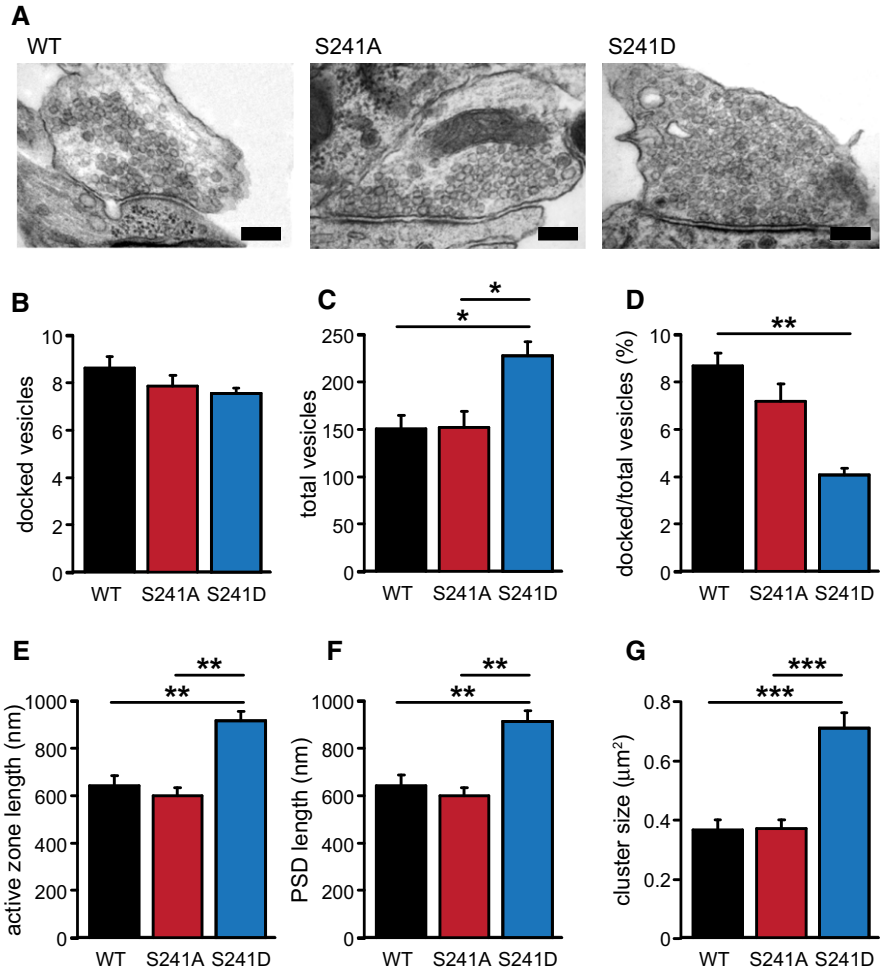

Figure EV3. Ultra-structural morphology of rescued Munc18-1 null mutant cells.

Related to Figure 4. Electron microscopy analysis of hippocampal autaptic neurons of Munc18-1 null mutant mice rescued with lentiviruses expressing $M18_{WT}$, $M18_{S241A}$, or $M18_{S241D}$. $N_{cultures} = 3$, $M18_{WT}$: $n_{cells} = 6$, $n_{synapses} = 138$; $M18_{S241A}$: $n_{cells} = 5$, $n_{synapses} = 146$; $M18_{S241D}$: $n_{cells} = 3$, $n_{synapses} = 77$. Synapses were averaged per cell. Graphs represent cell averages.

A Typical examples. Scale bar represents 200 nm.

B Mean number of docked vesicles ($M18_{WT}$: 8.64 ± 0.48; $M18_{S241A}$: 7.89 ± 0.44; $M18_{S241D}$: 7.57 ± 0.22, n.s., one-way ANOVA). $n = 3$.

C Mean number of total vesicles ($M18_{WT}$: 151.99 ± 14.28; $M18_{S241A}$: 152.65 ± 16.54; $M18_{S241D}$: 228.16 ± 15.86; $^*P < 0.05$, one-way ANOVA). $n = 3$.

D Percentage of docked vesicles out of total number of vesicles ($M18_{WT}$: 8.69 ± 0.55; $M18_{S241A}$: 7.20 ± 0.74; $M18_{S241D}$: 4.09 ± 0.28; $^{**}P < 0.01$, one-way ANOVA). $n = 3$.

E Mean active zone length ($M18_{WT}$: 643.12 ± 43.84 nm; $M18_{S241A}$: 601.62 ± 33.45 nm; $M18_{S241D}$: 918.24 ± 39.47 nm; $^{**}P < 0.01$, one-way ANOVA). $n = 3$.

F Mean postsynaptic density (PSD) length ($M18_{WT}$: 644.70 ± 43.74 nm; $M18_{S241A}$: 603.05 ± 33.49 nm; $M18_{S241D}$: 914.09 ± 47.52 nm; $^{**}P < 0.01$, one-way ANOVA). $n = 3$.

G Mean cluster size ($M18_{WT}$: 2.97 ± 0.15 µm²; $M18_{S241A}$: 3.00 ± 0.11 µm²; $M18_{S241D}$: 4.40 ± 0.23 µm²; $^{***}P < 0.001$, one-way ANOVA). $n = 3$.

Data information: Data are expressed as mean ± SEM.

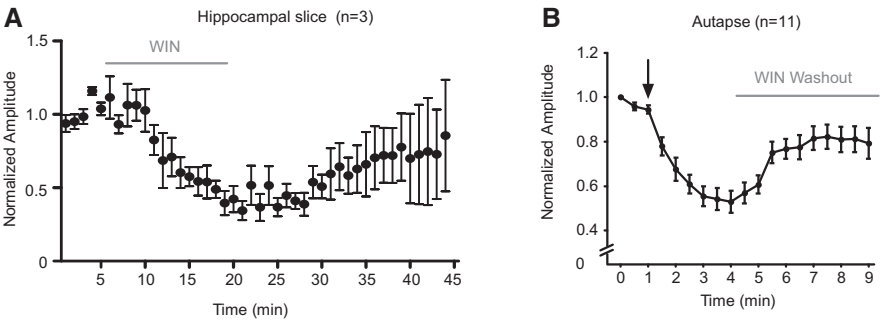

Figure EV4. WIN55,212-2-induced depression of transmission is reversible.

Related to Figure 7.

A Normalized EPSC amplitudes in hippocampal CA1 neurons during and after a 15-min application of 5 µM WIN55,212-2 (gray bar) shows the gradual recovery of EPSCs after WIN washout ($n = 3$ slices).

B Normalized EPSC amplitudes in wild-type hippocampal autapses during and after 30-s application of 1 µM WIN55,212-2 shows recovery during WIN washout (gray bar) ($n = 11$ neurons).

Data information: Data are expressed as mean ± SEM.

© 2016 The Authors

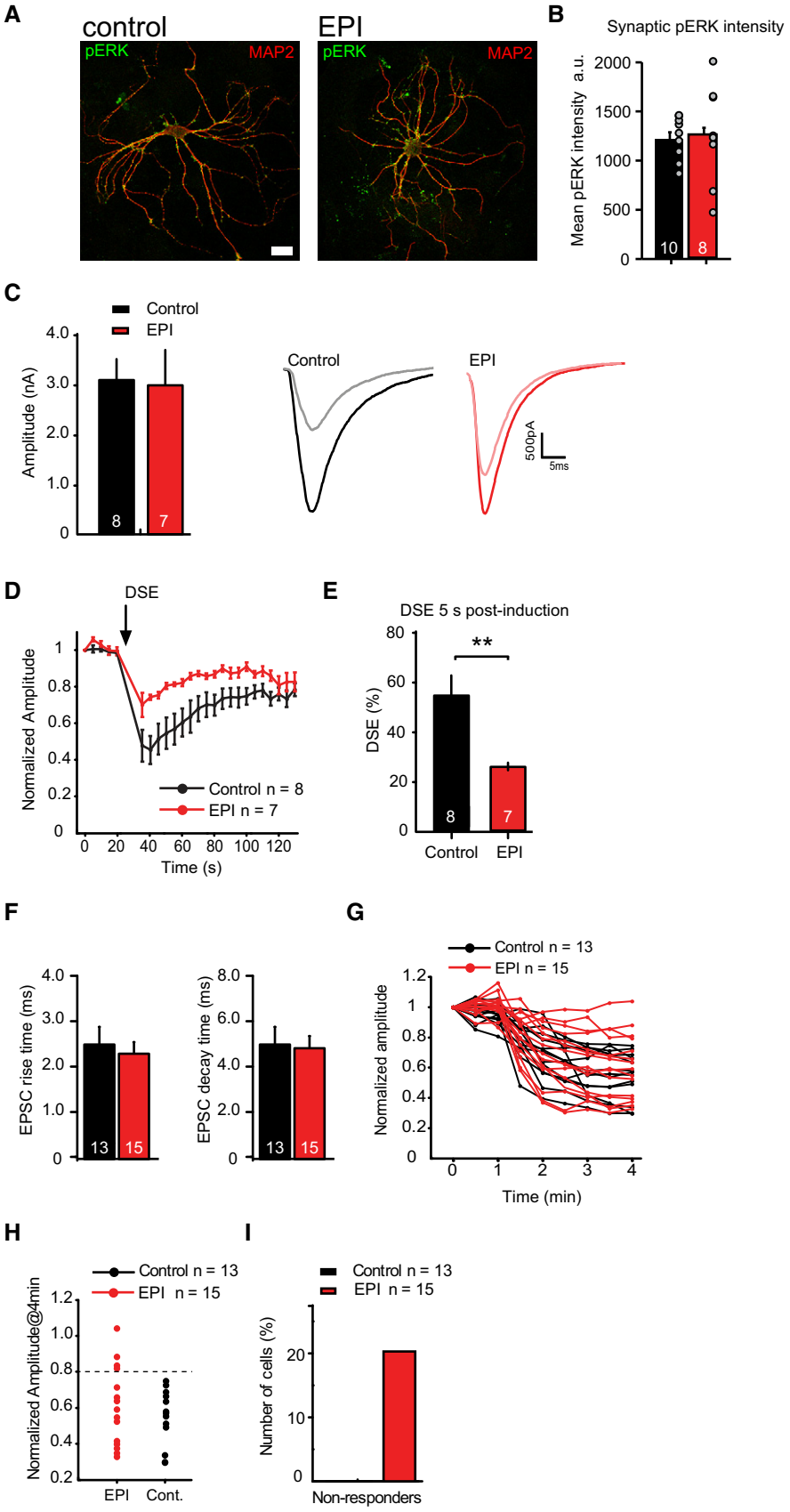

Figure EV5. ERK pathway inhibition decreases depolarization-induced suppression of excitation (DSE) and WIN55,212-2-induced depression in a subset of cultured neurons.

Related to Figure 7.

A Typical examples of isolated neurons pretreated with ERK inhibitors (EPI) or DMSO (control) for 3 h. Dendritic marker MAP2 (red), phospho-ERK antibody (pERK, green). Scale bar represents 10 μm.

B Semi-quantitative analysis of phospho-ERK intensities at synapses (identified by VAMP2, not shown) shows that pretreatment with ERK inhibitors does not result in reduction of phospho-ERK levels in all neurons (control n = 10 neurons, EPI n = 8 neurons). In these neurons, ERK appears to remain in a phosphorylated state much longer than in hippocampal slices (compare with Fig 3C).

C–E DSE duration and amplitude is decreased in hippocampal autaptic neurons upon ERK pathway inhibition compared to control. (C) Left: Average EPSC amplitude in wild-type autaptic neurons before a 10-s depolarizing pulse in control and ERK pathway inhibitors (EPI: 20 μM PD98059 and 10 μM U0126, applied 3 h before recordings) pretreated neurons is similar (control: 3.1 ± 0.4 nA, n = 8; EPI: 3.0 ± 0.7 nA, n = 7). Right: Examples of average EPSC traces for control (black and gray) and EPI (red and pink)-treated neurons prior to and after DSE, respectively. (D) Time course of normalized EPSC amplitudes recorded before and after a 10-s depolarizing pulse to 0 mV (DSE, indicated by the arrow) in wild-type autaptic neurons in the absence (control) or presence of ERK pathway inhibitors (EPI) (control n = 8, EPI n = 7 from 2 independent experiments). (E) DSE effect size in control and EPI-treated autapses 5 s after a 10-s depolarizing pulse to 0 mV (control n = 8, EPI n = 7, $^{**}P < 0.01$, Mann–Whitney U-test).

F–H ERK pathway inhibitors block effect of CB1 agonist WIN55,212-2 in a subset of hippocampal autaptic neurons. (F) EPSC rise and decay times of control (black bars) and EPI (red bars)-treated neurons prior to WIN55,212-2 application are similar. (G) Effect of 1 μM WIN application in individual cells after 4 min (start of application is at t = 1 min) in the absence (control, n = 13) and presence of ERK pathway inhibitors (EPI: 20 μM PD98059 and 10 μM U0126, applied 3 h before recordings, n = 15). (H) Normalized EPSC amplitudes 4 min after WIN application in control and EPI neurons. The dashed line represents cutoff used to distinguish non-responders (EPSC rundown < 20%) and responders (EPSC rundown > 20%) in (G).

I Ratio of non-responding versus responding neurons to 1 μM WIN application shows that in 20% of EPI-treated neurons, EPSC during WIN application remained above 80% of EPSC before WIN stimulation. In control cells, WIN application resulted in > 20% reduction of EPSCs in all neurons tested.

Data information: Data are expressed as mean ± SEM.

© 2016 The Authors